Department of Mathematics and Systems Analysis

Boundary shape analysis of electrical impedance tomography with applications

Stratos Staboulis

Aalto University

DOCTORAL DISSERTATIONS

Aalto University publication series
DOCTORAL DISSERTATIONS 141/2014

Boundary shape analysis of electrical impedance tomography with applications

Stratos Staboulis

A doctoral dissertation completed for the degree of Doctor of Science (Technology) to be defended, with the permission of the Aalto University School of Science, at a public examination held at the lecture hall M1 of the school on 17 October 2014 at 12.

Aalto University
School of Science
Department of Mathematics and Systems Analysis
Inverse Problems

Supervising professor
Prof. Nuutti Hyvönen

Thesis advisor
Prof. Nuutti Hyvönen

Preliminary examiners
Prof. Matti Lassas, University of Helsinki, Finland
Prof. Armin Lechleiter, Universität Bremen, Germany

Opponent
Prof. Daniela Calvetti, Case Western Reserve University, USA

Aalto University publication series
DOCTORAL DISSERTATIONS 141/2014

ISBN 978-952-60-5862-7
ISBN 978-952-60-5863-4 (pdf)
ISSN-L 1799-4934
ISSN 1799-4934 (printed)
ISSN 1799-4942 (pdf)
http://urn.fi/URN:ISBN:978-952-60-5863-4

Unigrafia Oy
Helsinki 2014

Finland

Aalto University

Abstract

Aalto University, P.O. Box 11000, FI-00076 Aalto www.aalto.fi

Author
Stratos Staboulis

Name of the doctoral dissertation
Boundary shape analysis of electrical impedance tomography with applications

Publisher School of Science

Unit Department of Mathematics and Systems Analysis

Series Aalto University publication series DOCTORAL DISSERTATIONS 141/2014

Field of research Mathematics

Manuscript submitted 10 June 2014 **Date of the defence** 17 October 2014

Permission to publish granted (date) 5 September 2014 **Language** English

☐ **Monograph** ☒ **Article dissertation (summary + original articles)**

Abstract

A typical *electrical impedance tomography (EIT)* reconstruction is ruined if the shape of the imaged body or the electrode locations are not accurately known. In this dissertation, a new approach based on (boundary) shape analysis is presented for online adaptation of the measurement geometry model.

It is shown that the forward operator of the *complete electrode model (CEM)* of EIT is *Fréchet differentiable* with respect to both the outer boundary shape of the object and the electrode locations. A dual technique allows feasible computation of the gradients in a Newton-type 'output least squares' algorithm for the simultaneous reconstruction of the conductivity and the measurement geometry. Shape calculus techniques are also applied to optimal experiment design for EIT. To be more precise, numerical optimization of the electrode positions is carried out with respect to posterior covariance related criteria derived from the Bayesian inversion paradigm.

Special attention is paid to the Sobolev regularity properties of the CEM essential for the shape analysis. By interpolation of Sobolev spaces it is proven that the CEM is a perturbation of the less regular *shunt model* of EIT. Consequently, instability in the computation of the numerical shape derivative can be expected if the contact resistances are small.

Keywords Inverse problems, electrical impedance tomography, complete electrode model, shape analysis, optimal experimental design, Bayesian inversion, elliptic boundary value problems, mixed bounday conditions

ISBN (printed) 978-952-60-5862-7 **ISBN (pdf)** 978-952-60-5863-4

ISSN-L 1799-4934 **ISSN (printed)** 1799-4934 **ISSN (pdf)** 1799-4942

Location of publisher Helsinki **Location of printing** Helsinki **Year** 2014

Pages 154 **urn** http://urn.fi/URN:ISBN:978-952-60-5863-4

A! Aalto-yliopisto

Tiivistelmä

Aalto-yliopisto, PL 11000, 00076 Aalto www.aalto.fi

Tekijä
Stratos Staboulis

Väitöskirjan nimi
Reunanmuotoanalyysin sovelluksia impedanssitomografiaan

Julkaisija Perustieteiden korkeakoulu

Yksikkö Matematiikan ja systeemianalyysin laitos

Sarja Aalto University publication series DOCTORAL DISSERTATIONS 141/2014

Tutkimusala Matematiikka

Käsikirjoituksen pvm 10.06.2014 **Väitöspäivä** 17.10.2014

Julkaisuluvan myöntämispäivä 05.09.2014 **Kieli** Englanti

☐ **Monografia** ☒ **Yhdistelmäväitöskirja (yhteenveto-osa + erillisartikkelit)**

Tiivistelmä

Impedanssitomografiassa (EIT) kappaleen reunanmuodon ja elektrodien sijaintien epätarkka mallinnus pilaa tavallisesti johtavuuden rekonstruktion. Väitöskirjassa esitellään uusi (reunan)muotoanalyysiin perustuva menetelmä, joka mahdollistaa mittausgeometrian reaaliaikaisen sovittamisen dataan.

Työssä osoitetaan, että EIT:n *täydellisen elektrodimallin (CEM)* suoran ongelman ratkaisu on *Fréchet-derivoituva* sekä kappaleen reunanmuodon että elektrodien sijaintien suhteen. Johtavuusjakauma ja mittausgeometria rekonstruoidaan yhtäaikaisesti Newton-tyyppisellä neliösumman minimointialgoritmilla. Tarvittavat gradientit voidaan laskea tehokkaasti duaalitekniikan avulla. Muotoanalyyttisiä menetelmiä sovelletaan myös optimaalisen EIT-mittauksen suunnitteluun, missä elektrodien sijainnit optimoidaan numeerisesti posteriorikovarianssiin liittyvien Bayesiläisten kriteerien mukaisesti.

Erityistä huomiota kiinnitetään CEM:n Sobolev-säännöllisyysominaisuuksiin, jotka ovat olennaisia työssä sovelletun muotoanalyysin kannalta. Sobolev-avaruuksien välisellä interpolaatiolla osoitetaan, että CEM on perturboitu versio eräästä ideaalisesta elektrodimallista (*shunt*-malli). Tästä tuloksesta voidaan päätellä muotoderivaattojen numeerisen approksimoinnin epästabiilius, mikäli kontaktiresistanssit ovat pieniä.

Avainsanat Inversio-ongelmat, impedanssitomografia, täydellinen elektrodimalli, muotoanalyysi, optimaalinen kokeiden suunnittelu, Bayesiläinen inversio, elliptiset reuna-arvo-ongelmat, sekareunaehdot

ISBN (painettu) 978-952-60-5862-7 **ISBN (pdf)** 978-952-60-5863-4

ISSN-L 1799-4934 **ISSN (painettu)** 1799-4934 **ISSN (pdf)** 1799-4942

Julkaisupaikka Helsinki **Painopaikka** Helsinki **Vuosi** 2014

Sivumäärä 154 **urn** http://urn.fi/URN:ISBN:978-952-60-5863-4

Preface

This study was carried out at the Department of Mathematics and Systems Analysis at Aalto University during 2011–2014. I acknowledge the funding provided by the Academy of Finland.

I express my deepest gratitude to Nuutti Hyvönen for being an excellent thesis instructor. His advice was always sharp, and — even when busy — he was generous with his time. Special thanks are also due to Aku Seppänen and Jérémi Dardé for collaboration and hosting during research visits. In addition, I am grateful to all members of the Inverse Problems research group at Otaniemi for sharing interesting thoughts, and creating an inspiring working atmosphere.

For the careful pre-examination of this dissertation and the valuable comments, I am indebted to Matti Lassas and Armin Lechleiter. Moreover, it is an honour to have Daniela Calvetti as the opponent in my thesis defense.

Finally, I would like to thank my family for their continuous support and encouragement, my friends for the wonderful moments we have spent together, and my dear partner Outi for being in my life and helping me through difficult times.

Helsinki, September 11, 2014,

Stratos Staboulis

Contents

List of Publications

This thesis consists of an overview and of the following publications which are referred to in the text by their Roman numerals.

[**I**] Dardé, J., Hakula, H., Hyvönen, N., and Staboulis, S. Fine-tuning electrode information in electrical impedance tomography. *Inverse Problems and Imaging*, 6(3):399–421, 2012.

[**II**] Dardé, J., Hyvönen, N., Seppänen, A., and Staboulis, S. Simultaneous reconstruction of outer boundary shape and admittivity distribution in electrical impedance tomography. *SIAM Journal on Imaging Sciences*, 6(1):176–198, 2013.

[**III**] Dardé, J., Hyvönen, N., Seppänen, A., and Staboulis, S. Simultaneous recovery of admittivity and body shape in electrical impedance tomography: An experimental evaluation. *Inverse Problems*, 29(8):085004, 2013.

[**IV**] Dardé, J., and Staboulis, S. Electrode modelling: The effect of contact impedance. *arXiv:1312.4202*, 20 pages, 2013.

[**V**] Hyvönen, N., Seppänen, A., and Staboulis, S. Optimizing electrode positions in electrical impedance tomography. Accepted to *SIAM Journal on Applied Mathematics, arXiv:1404.7300v2*, 22 pages, 2014.

Author's Contribution

The author contributed substantially to the writing process of all five articles:

Publication I: "Fine-tuning electrode information in electrical impedance tomography"

The author made a major contribution to both the theoretical results (part of which originates from his Master's thesis [51]) and the numerical approximation of the Fréchet derivative. The incorporation of the geometric component into the solver is due to the author.

Publication II: "Simultaneous reconstruction of outer boundary shape and admittivity distribution in electrical impedance tomography"

Most of the mathematical analysis and the numerical approximation of the Fréchet derivative are due to the author. The incorporation of the geometric component into the three dimensional solver (provided by Seppänen) was carried out by the author.

Publication III: "Simultaneous recovery of admittivity and body shape in electrical impedance tomography: An experimental evaluation"

The author took part in the laboratory experiments at the University of Eastern Finland in Kuopio. The used algorithm is an adaptation of the one in [**I**, **II**]. The suitable modifications and numerical computations

are all due to the author.

Publication IV: "Electrode modelling: The effect of contact impedance"

Most of the theoretical results and all the numerical experiments were developed by the author. This work is based on discussions with Dardé in Toulouse during June 2013.

Publication V: "Optimizing electrode positions in electrical impedance tomography"

A large part of the theory and all the numerical computations are due to the author.

1. Introduction

In *Electrical Impedance Tomography* (EIT), the aim is to extract information about the internal properties of a physical object by external measurements of electric current and voltage. In practice, through a set of surface electrodes, currents of prescribed magnitudes are conducted into the object and the voltages needed for maintaining the currents are recorded. This procedure is often repeated with several different input current patterns. Afterwards, the obtained current-voltage data are used to compute an image of the interior of the object. Typically, the image represents an estimate of the electrical *conductivity* (or more generally *admittivity*) distribution of the object.

In many situations the conductivity distribution may carry valuable information about the examined object. For instance, the conductivities of air, blood, cancer tissue and healthy tissue can differ significantly from each other at human body temperature. This fact is utilized in EIT-based breast cancer detection or real-time monitoring of lung function. Examples of non-clinical EIT applications include, among others, control of industrial processes, non-destructive testing of materials and locating mineral deposits. For more details about the potential uses of EIT, consult the review articles [8, 13, 56] and the references therein.

Compared to conventional imaging modalities such as *X-ray computed tomography* (CT) or *magnetic resonance imaging* (MRI), EIT enables inexpensive and easily portable equipment. Moreover, EIT is relatively safe because the applied currents are typically of low magnitude, and the electrical measurements do not expose the subject to ionizing radiation (such as X-rays). In contrast to CT or MRI, EIT images are characterized by low spatial resolution (but high temporal resolution) making it ill-suited for imaging detailed structures.

The lack of spatial resolution in EIT imaging is explained by the *ill-posed* nature of the inverse conductivity problem; even with high number of electrodes, the strong diffusion of electric potential by conductive medium has the effect that very different conductivity distributions can cause practically indistinguishable electrode voltages. Therefore, a typical set of noisy EIT measurement data contains only very limited information about the underlying conductivity distribution. For this reason, even relatively small amounts of noise or modelling error can severely deteriorate the image quality.

Especially *absolute EIT* imaging (where the data corresponds to a single conductivity distribution) is notorious for its sensitivity to mismodelling of the electrode positions and the shape of the object. In a typical reconstruction algorithm, even a slight imprecision in the measurement geometry usually leads to ruined conductivity images. This is a major drawback of absolute EIT as a biomedical imaging technique since, in practice, the precise electrode locations and/or object shape are rarely known. The main research problem of the dissertation is *(i) to develop a framework for practical 2D & 3D absolute EIT reconstruction algorithms that tolerate uncertainty in the measurement geometry.*

Besides being a source of modelling error, the EIT measurement geometry (or more relevantly the electrode configuration) can affect the conductivity information content of the EIT measurement. For example, if one is interested only in imaging a subregion of the object, it makes sense to position the electrodes so that the current can be concentrated to that region. Also, particularly in real-time monitoring of some rapidly varying processes, there may not be enough time to perform exhaustive current-voltage measurements. Under such circumstances, it is desirable to configure the electrodes optimally based on the available prior information. The second research problem of this thesis is *(ii) to build a paradigm for optimizing electrode positions in absolute EIT.*

Outline of the dissertation

According to experimental studies [14, 49] the so-called *complete electrode model* (CEM) of EIT is capable of predicting electrode voltages up to the measurement precision. We hypothesize that, in absolute EIT, the

geometric modelling error can be reduced significantly by reconstructing the measurement geometry and the conductivity distribution simultaneously within the CEM framework. Most EIT algorithms capable of producing conductivity reconstructions from absolute experimental data model the measurements using the CEM, and rely on Newton-type minimization of an 'output least squares' functional [13]. Although such an approach cannot be considered extremely sophisticated mathematically, it provides a flexible framework to incorporate the electrode positions and the outer boundary shape as a part of the reconstruction. To make this approach feasible, an efficient method for numerically differentiating the output functional with respect to the geometric attributes is needed.

In the first two articles of the dissertation, a *shape gradient* of the electrode voltages (modelled by the CEM) is determined. The shape gradient is shown to consist of two components corresponding to the electrode locations [**I**] and the outer boundary shape [**II**], respectively. It is further demonstrated that these components can be numerically implemented in the computation of the needed derivatives in a Gauss–Newton-like reconstruction algorithm for both simulated and experimental EIT data.

The shape analysis of the CEM relies on the Sobolev regularity of the corresponding spatial potential distribution. The sufficient regularity is guaranteed by the contact resistance parameters which are used in the CEM to describe the quality of contacts at the electrode/object interfaces. However, for close-to-vanishing contact resistance (perfect contacts), instability in the used finite element approximation of the shape gradient is observed [**III**]. The theoretical basis for this effect is developed in [**IV**]. It is shown that, when the contact resistances tend to zero, the CEM forward solution converges to a function without the required regularity.

The derived shape analysis also provides feasible tools for the optimization of electrode positions in EIT. In paper [**V**], an application of the shape gradient in optimal experiment design of EIT is presented. To be more precise, the electrode positions are optimized with respect to certain criteria derived from Bayesian statistics.

2. Electrical Impedance Tomography

In this section we present a brief survey of the mathematical fundamentals of EIT; for a more detailed introduction to this broad topic, the reader is advised to consult [8, 13, 56] and the references therein.

In classical electrostatics, the absence of current sinks and sources in an isotropic conductive medium can be expressed by the *conductivity equation*

$$\nabla \cdot (\sigma(x)\nabla u(x)) = 0, \tag{2.1}$$

where $\sigma = \sigma(x) > 0$ and $u = u(x)$ model the spatial conductivity distribution and the electric potential, respectively. The most important models for EIT are formulated using boundary value problems for (2.1) or its generalizations to time-harmonic fields and/or anisotropic (matrix-valued) conductivities. In the time-harmonic case, an equation of form (2.1), with σ replaced by a complex valued *admittivity*, can be derived from Maxwell's equations using approximations that are justified for the frequency range within which EIT typically operates. In the following, it is assumed that σ is real-valued unless mentioned otherwise.

2.1 Continuum model

Most of the theory related to EIT is based on the *continuum model* which assumes infinite dimensional boundary data. Let $\Omega \subset \mathbb{R}^d$, $d = 2, 3$, be a domain describing the dimensions of the object of interest; the boundary of Ω is abbreviated by Γ and assumed to be smooth enough. The set of admissible conductivities is denoted by

$$L^\infty_+(\Omega) = \Big\{ \sigma \in L^\infty(\Omega) \ : \ \operatorname{ess\,inf}_{x\in\Omega} \sigma(x) > 0 \Big\}. \tag{2.2}$$

The formal idea is that if a current density f is applied on Γ, then the electric potential u in Ω is governed by the Neumann boundary value problem

$$\nabla \cdot (\sigma \nabla u) = 0 \quad \text{in} \quad \Omega, \qquad \sigma \frac{\partial u}{\partial \nu} = f \quad \text{on} \quad \Gamma, \tag{2.3}$$

where ν is the outward unit normal of Γ. A straightforward application of the theory of elliptic partial differential equations shows that for any given

$$f \in H_\diamond^{-1/2}(\Gamma) = \{f \in H^{-1/2}(\Gamma) \,:\, \langle f, 1\rangle = 0\},$$

the problem (2.3) has a solution $u \in H^1(\Omega)$ that is unique up to an additive constant. Here the angular brackets denote the dual pairing between $H^{-1/2}(\Gamma)$ and $H^{1/2}(\Gamma)$; note also that the 'zero-mean' property of f corresponds to the current conservation law.

An ideal set of (static) EIT measurement data would correspond to the knowledge of the full set of Cauchy data

$$\left\{(f, u|_\Gamma) \,:\, u \text{ solves (2.3) for } f \in H_\diamond^{-1/2}(\Gamma)\right\}$$

which is characterized by the *Neumann-to-Dirichlet map*

$$\Lambda_\sigma : H_\diamond^{-1/2}(\Gamma) \to H^{1/2}(\Gamma)/\mathbb{R}, \qquad \Lambda_\sigma f = u|_\Gamma,$$

where $u|_\Gamma$ is the Dirichlet trace of the solution to (2.3). It is not hard to show that Λ_σ is a positive definite and self-adjoint linear isomorhpism, with its inverse Λ_σ^{-1} being the corresponding *Dirichlet-to-Neumann map*. Note that although Λ_σ is linear, the mapping $\sigma \mapsto \Lambda_\sigma$, which relates the conductivity to the ideal boundary measurements, is non-linear.

The purely theoretical version of the inverse conductivity problem of EIT can be formulated as *'Is it possible to determine the conductivity σ from the knowledge of Λ_σ?'*; the fundamental results on this topic are listed in the following section. However, it is advisable to keep in mind that although the continuum model is mathematically well-established, it is a bad model for real-life electrode measurements [14, 49]. Therefore, other models are needed in practice.

2.2 Inverse conductivity problem

The inverse conductivity problem has been extensively studied in dimensions $d \geq 2$ ever since the publication of [11] by A. Calderón; this is

why the inverse conductivity problem is often called *Calderón problem*. It is known that for large classes of isotropic (real-valued) conductivities there is a one-to-one correspondence between σ and Λ_σ [4, 35, 43, 54, 56] whereas for anisotropic (matrix-valued) conductivities the same does not hold. Note that although many of the uniqueness proofs use constructive techniques, they do not necessarily imply numerical schemes for the estimation of σ. The question of reconstructing (information about) σ from boundary measurements is considered in §2.4.

Interestingly, the minimal assumptions on σ and Ω for the existing uniqueness proofs are different for $d = 2$ and $d \geq 3$ spatial dimensions. In the plane, unique determination of σ by Λ_σ has been shown for any real-valued $\sigma \in L^\infty_+(\Omega)$ and a general domain Ω with a connected complement [4], whereas in $d \geq 3$, some extra regularity is required from both σ and Γ [9, 22, 46]. It should also be mentioned that there exists a variety of *partial data* results where Cauchy data pairs for the conductivity equation are assumed known on a subset $\Gamma' \subset \Gamma$, and still, identifiability for general classes of conductivities can be deduced [28, 31].

In the case of an anisotropic conductivity σ, there is no uniqueness because deforming Ω by a boundary preserving diffeomorphism Φ yields another anisotropic conductivity $\tilde{\sigma} = \Phi_* \sigma$ with $\Lambda_{\tilde{\sigma}} = \Lambda_\sigma$ (see e.g. [52]). In the plane the converse also holds true, thus fully characterizing the non-uniqueness [2, 52]. In dimensions $d \geq 3$, the non-uniqueness can be characterized to a certain extent [21, 37].

Before concluding the section, we consider briefly the instability of the inverse conductivity problem. It can be shown [1] that even if the inverse map $\Lambda_\sigma \mapsto \sigma$ existed, it would be discontinuous from (a subset of) the space of linear operators $\mathcal{L}(H^{-1/2}(\Gamma), H^{1/2}(\Gamma))$ to $L^\infty(\Omega)$. With sufficient smoothness constraints on the conductivity, a logarithmic modulus of continuity between the aforementioned topologies can, however, be obtained [1, 6]. For more information on the (in)stability results for the inverse conductivity problem, we refer to [56].

2.3 Complete electrode model

In practice, the EIT data is collected by M contact electrodes on the surface of the object. The CEM is an accurate model for real-life mea-

surements because it takes into account the electrode shapes and the imperfect contacts between the object and the electrodes.

Because electrodes are usually made of a highly conductive material, in the CEM they are modelled as ideal conductors. In other words, the electric potential on an electrode is assumed to be a constant that can be measured. In real world, the current density under the electrode is unknown, but the net electrode currents can be controlled. On the other hand, hardly any current penetrates the object boundary outside the electrodes in a typical EIT measurement environment. Furthermore, it can be argued [14, 49] that the contact between the electrodes and the surface of the object is not perfect. This effect can be modelled as thin resistive layers, with a surface resistance $z_m > 0$, at the electrode/object interfaces. The conductivity equation (2.1) combined with the above features gives rise to the boundary value problem

$$\begin{aligned} &\nabla \cdot (\sigma \nabla u) = 0 && \text{in } \Omega, \\ &\sigma \frac{\partial u}{\partial \nu} = 0 && \text{on } \Gamma \setminus \bigcup_{m=1}^{M} E_m, \\ &u + z_m \sigma \frac{\partial u}{\partial \nu} = U_m && \text{on } E_m, \\ &\int_{E_m} \sigma \frac{\partial u}{\partial \nu} \, \mathrm{d}S = I_m, && m = 1, 2, \ldots, M. \end{aligned} \tag{2.4}$$

It is not hard to demonstrate that for any given $I = \{I_m\}_{m=1}^M \in \mathbb{R}_\diamond^M$, (2.4) has a unique solution (u, U) in the space $(H^1(\Omega) \oplus \mathbb{R}^M)/\mathbb{R}$. Here $\mathbb{R}_\diamond^M \subset \mathbb{R}^M$ is the subspace of vectors whose entries sum up to zero. The second component U models the electrode voltages. The CEM, that is (2.4), has been shown to be capable of reproducing measurement data reasonably well (at best up to .1% [49]).

The electrode measurement map corresponding to (2.4), defined via

$$R_{\sigma,z} I = U, \qquad R_{\sigma,z} : \mathbb{R}_\diamond^M \to \mathbb{R}^M/\mathbb{R}, \tag{2.5}$$

is invertible and can be represented as a symmetric $\mathbb{R}^{(M-1)\times(M-1)}$ matrix [49]. Consequently, there are only $M(M-1)/2$ degrees of freedom in $R_{\sigma,z}$, which is certainly not enough information for uniquely determining a general conductivity.

Many (theoretical) EIT reconstruction algorithms require an approximation of Λ_σ as an input. Thus, it is important to understand the relationship between $R_{\sigma,z}$ and Λ_σ. Under reasonable assumptions, it can

be shown [26] that the composition of $R_{\sigma,z} - \mathrm{diag}(z)$ with suitable projections converges in $\mathcal{L}(L^2_\diamond(\Gamma), L^2(\Gamma)/\mathbb{R})$ to the compact operator

$$\Lambda_\sigma : L^2_\diamond(\Gamma) \to L^2(\Gamma)/\mathbb{R}$$

as the maximal distance between the centers of adjacent electrodes tends to zero, that is, when the number of electrodes is increased and their size decreased in a controlled manner.

2.4 Reconstruction methods

The practical version of the inverse conductivity problem is as follows: given a discrete set of (noisy) electrode measurements, reconstruct an image of the conductivity inside the examined object. The existing EIT reconstruction methods fall roughly into two categories: *iterative* and *direct* algorithms. Due to the ill-posedness of the underlying inverse problem, all the functional reconstruction methods involve some form of regularization which enables stable reconstruction. Often, the regularization has an interpretation in terms of the available prior information on the unknown parameters [29, 30].

Most real-life applications of EIT employ iterative methods based on data-fitting by minimizing an 'output least squares' discrepancy functional over a set of admissible conductivities (and other model parameters). Regularization can be achieved via adding suitable penalty terms to the cost functional or, e.g., by suitable stopping criteria for Krylov subspace methods [40]. Due to the non-linearity of the problem, the minimization typically involves (gradient-based) Newton-type steps. Examples of iterative EIT reconstruction algorithms can be found in [12, 39, 57, 59] and the references therein. Also other than 'discrepancy' type objective functionals have been considered; see e.g. [8] for an approach based on variational principles.

The iterative methods are attractive because their implementation does not require deep understanding of the fine aspects of the forward model. Thus it is possible to directly use an accurate forward model such as the CEM. Moreover, the incorporation of prior information is usually straightforward. Although these methods can be tuned to yield very good reconstructions, there are several disadvantages, too. In most cases, there

is no proof of convergence, and the relationship between the reconstruction and the 'true' conductivity is not well-understood. Furthermore, especially in three-dimensional imaging, the computational workload can become overwhelming.

The methods that do not involve recursive iterations are here classified as direct. Perhaps the most fundamental technique in two dimensions is the $\overline{\partial}$ *(D-bar) -method* [42] which implements the constructive two-dimensional uniqueness proof in [43] (see also [3] for a direct EIT reconstruction method based on the uniqueness proof in [4]). Under certain conditions, a variant of the $\overline{\partial}$-method admits a *regularization strategy* [34], that is, the reconstruction converges to the true conductivity as the noise level tends to zero; this kind of a property is not known for any (non-trivial) iterative EIT method.

Other proposed direct methods include the *Calderón's linearization method* [11, 42] and the *layer stripping algorithm* [50, 53]. Moreover, sampling type methods that aim at *locating* (the supports of) conductivity inhomogeneities in a known background [10, 33, 38] allow a very fast reconstruction. In practice, many direct methods can be difficult to implement because they typically require difference data as the input. Moreover, it is not usually known how to include detailed prior information in the direct reconstruction algorithms.

2.5 Modelling error

It is known that the choice of the measurement model can affect the predicted EIT data more than major changes in the conductivity distribution; see e.g. [47] for a numerical study on this subject. Even when the CEM is used, significant modelling errors may arise from uncertainty about some other model parameters such as the electrode locations, the contact resistances, or the shape of the imaged object. It is well-known that even slight perturbations in these attributes can cause major artefacts in reconstructions [**I**, **II**, **III**]; a simulation of this effect is illustrated in Figure 2.1.

A conventional trick to improve the tolerance of modelling errors is to apply reconstruction methods working with *difference data* $U - \tilde{U}$, that is, the difference between EIT measurements corresponding to two dif-

ferent conductivities σ and $\tilde{\sigma}$ (or admittivities in the case of frequency difference data). It has been observed that, if the measurement geometry and contact resistances remain unperturbed, part of the modelling error is removed in the difference data; see Figure 2.2 for a simulation of this phenomenon. Unfortunately, this may fail e.g. in medical applications due to orientation shifts or breathing of the patient. At worst, the relative error may even be amplified in the difference data for the following reason. Let $U^\varepsilon = U + \varepsilon$ and $\tilde{U}^{\tilde{\varepsilon}} = \tilde{U} + \tilde{\varepsilon}$ be noisy measurements corresponding to two different conductivities with ε and $\tilde{\varepsilon}$ being realizations of independent zero mean random variables, whence $\mathbb{E}|\varepsilon - \tilde{\varepsilon}|^2 = \mathbb{E}|\varepsilon|^2 + \mathbb{E}|\tilde{\varepsilon}|^2$. By ill-posedness, changes in the conductivity may not affect the data much, meaning that $|U - \tilde{U}| \ll |U|, |\tilde{U}|$. Therefore the relative (squared) mean error in the difference data $\mathbb{E}|\varepsilon - \tilde{\varepsilon}|^2/|U - \tilde{U}|^2$ may be augmented, especially if $\mathbb{E}|\varepsilon|^2 = c|U|^2$ and $\mathbb{E}|\tilde{\varepsilon}|^2 = \tilde{c}|\tilde{U}|^2$ for some constants $c, \tilde{c} > 0$.

The problems with modelling errors in absolute EIT have been partly resolved in earlier works. It is possible to include the estimation of contact resistances as a part of an iterative reconstruction algorithm [59]. Furthermore, two successful approaches to coping with unknown exterior boundary shape have been introduced prior to this dissertation. The method in [36] is based on allowing anisotropic conductivities to account for the domain distortion. In [44, 45], the errors resulting from an incorrect boundary shape are compensated using the so-called *approximation error approach* where the idea is to represent the modelling error as an additive stochastic term whose (second order) statistics are approximated via simulations.

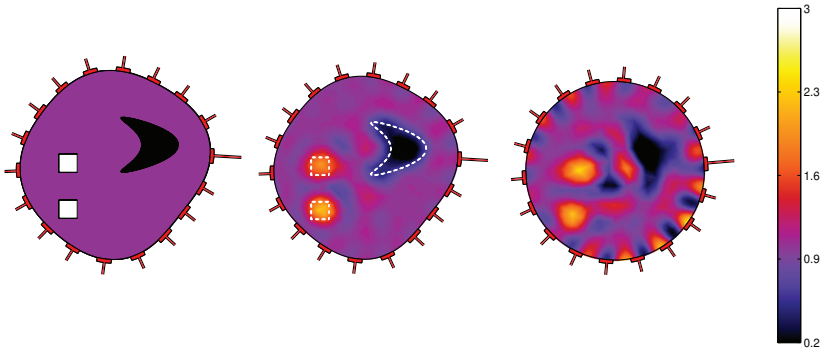

Figure 2.1. 2D *absolute* EIT reconstructions with (middle) exactly known and (right) mismodelled measurement geometries. The measurement data, which is corrupted by 0.9‰ relative noise, is simulated using the object depicted on left. The contact resistances $z_m = 0.1$, $m = 1, \ldots, 18$ are assumed to be known. For more information on the employed Newton-type reconstruction algorithm, see e.g. the publications [**II**, **III**] and the references therein.

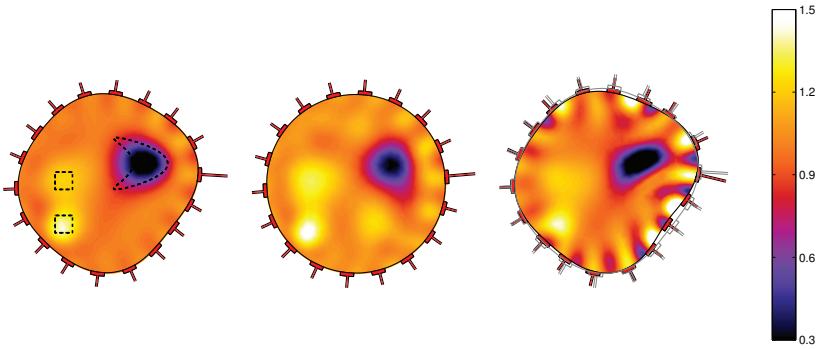

Figure 2.2. 2D *difference* EIT reconstructions with different a priori assumptions on the geometry. The measurement $\tilde{U}^{\tilde{\varepsilon}}$ is simulated using the object depicted on left in Figure 2.1, whereas the shape of the domain (with homogeneous unit conductivity) employed in the generation of the reference measurement U^{ε} varies. Both $\tilde{U}^{\tilde{\varepsilon}}$ contain 0.9‰ of relative noise. The first two reconstructions (from left) correspond to the case where $\tilde{U}^{\tilde{\varepsilon}}$ is simulated using exact geometry; the reconstructions are computed in (left) the exactly known and (middle) the mismodelled geometry. On right, both the simulation of the reference measurement U^{ε} and the reconstruction are performed using a slightly mismodelled geometry (the exact geometry is visualized by the gray line); this illustrates a situation where difference EIT may fail. In this case, the difference data contains a remarkable amount of 10% of relative noise due to the reasons explained in §2.5. In all computations, the contact resistances are assumed to have the known values $z_m = 0.1$, $m = 1, \ldots, 18$. The used Newton-type algorithm is formulated directly for difference data; otherwise it is analogous to the one of Figure 2.1.

3. Differentiability of EIT models with applications

The differential calculus for forward models has important applications in inverse problems, particularly in iterative reconstruction algorithms. In normed vector spaces there exist several notions of a derivative. Perhaps the most fundamental is the *Fréchet derivative* defined as follows: Let $\mathcal{H}_1$, $\mathcal{H}_2$ be normed vector spaces, $\mathcal{G} \subset \mathcal{H}_1$ open and $F : \mathcal{G} \to \mathcal{H}_2$. The operator F is said to be *Fréchet differentiable* at $\eta \in \mathcal{G}$ if there exists a linear map $F'(\eta) : \mathcal{H}_1 \to \mathcal{H}_2$ such that

$$\lim_{0 \neq \varepsilon \to 0} \frac{\|F(\eta + \varepsilon) - F(\eta) - F'(\eta)\varepsilon\|_{\mathcal{H}_2}}{\|\varepsilon\|_{\mathcal{H}_1}} = 0; \tag{3.1}$$

the operator $F'(\eta)$ is called the Fréchet derivative of F at $\eta \in \mathcal{H}_1$. It is easy to demonstrate that F' obeys familiar laws, such as the chain rule. Fréchet differentiability is a very strong property; many optimization methods can be implemented using the weaker *Gateaux derivative* [16, 17] which also exhibits many of the desired elements of classical differential calculus.

As discussed in §2.4, EIT reconstruction methods based on linearizations of the forward maps $F(\sigma) = \Lambda_\sigma$ or $F(\sigma, z) = R_{\sigma,z} I$ are common. In the pioneering paper [11] it was proven for $F(\sigma) = \Lambda_\sigma$ that $F'(\sigma)|_{\sigma=\text{const}}$ is injective on $L^\infty(\Omega)$. This, in a certain sense, justifies the detection of small conductivity perturbations using the linearized forward operator. In fact the linearization can provide substantial information even if the perturbation is not small; if a solution $\kappa \in L^\infty(\Omega)$ to the equation $F(\sigma) - F(\sigma_0) = F'(\sigma_0)\kappa$ exists, then κ contains essential information on the support of $\sigma - \sigma_0 \in L^\infty(\Omega)$ [23].

3.1 Generic Newton-type iterative algorithms

The penalized minimization problem

$$\arg\min_{\eta\in\mathcal{K}} J(\eta), \qquad J(\eta) = \|F(\eta) - V\|^2_{\mathcal{H}_2} + P(\eta) \tag{3.2}$$

can be motivated by its regulative properties [19, 32] or starting from the statistical context [30]. Here V is the measured data, $\mathcal{K} \subset \mathcal{H}_1$ is a set of admissible model parameters and $P : \mathcal{H}_1 \to [0, \infty)$ is a penalty functional. In the classical regularization theory, questions such as 'is (3.2) solvable?', and 'if it is, does it admit a regularization strategy?' are studied. For a linear F and quadratic penalization, the theory is well established [19]. For a non-linear F, no comprehensive theory exists although a part of the linear regularization theory extends to the non-linear case if the Fréchet derivative F' is regular enough. However, in the context of EIT, no regularization strategy for (3.2)-type methods (without extensive restrictions on the conductivity) is known. For literature on classical regularization theory, see [19, 32, 41, 55] and the references therein.

In practice $\mathcal{H}_1, \mathcal{H}_2$ are usually Hilbert spaces. If F and P are sufficiently many times Fréchet differentiable, iterative methods may be able to solve (3.2). A standard (second order) optimization algorithm is given by the *Newton's method* [60] defined as

$$\eta_{j+1} = \eta_j - (\operatorname{Hess} J(\eta_j))^{-1} \operatorname{Grad} J(\eta_j) \tag{3.3}$$

where

$$\operatorname{Grad} J(\eta) = 2F'(\eta)^*(F(\eta) - V) + \operatorname{Grad} P(\eta)$$

and

$$\operatorname{Hess} J(\eta) = 2F'(\eta)^*F'(\eta) + 2F''(\eta)^*(F(\eta) - V) + \operatorname{Hess} P(\eta)$$

are the gradient and the Hessian of the cost function J, respectively. Note that if all the relevant operators are bounded, then (by Lax–Milgram theorem [15]) positive definiteness of $\operatorname{Hess} J(\eta)$ is sufficient condition for its invertibility. Under suitable regularity assumptions, the Newton's method converges at a quadratic rate if the initial guess is sufficiently good [60].

In practice, the computation of $F''(\eta)^*$ can be tedious. A more feasible alternative of (3.3) is provided by the *Gauss–Newton (G–N)* method, where the term involving F'' is neglected. In addition, to further simplify the computations, the penalty term is often chosen to be quadratic, i.e., $P(\eta) = \|L(\eta - \eta_0)\|^2_{\mathcal{H}_3}$ where $L : \mathcal{H}_1 \to \mathcal{H}_3$ is linear. The performance of the G–N method (and the Newton's method) can be improved by, e.g., adaptive choice of the step size via line search and/or *Levenberg–Marquardt* modifications [60]. There exist also studies on the convergence of a generic G–N algorithm [5, 7].

3.2 Applications in EIT reconstruction

G–N-type optimization methods have been successfully applied to the estimation of both σ and z from experimental data [13, 24, 42, 58]. Note that the successive linearizations are justified by the fact that $F(\sigma, z) = R_{\sigma,z}I$ is (infinitely many times) Fréchet differentiable in $L^\infty(\Omega) \oplus (0, \infty]^M$ [11, 59], and the Hilbert space structure required in (3.3) is achieved via discretization of $L^\infty_+(\Omega)$. Although regulative properties of such methods are not well-understood, the local convergence of a discretized CEM-based (inexact) Newton-like algorithm has been established in [40]; see also [18] for a (theoretical) study on the convergence of a G–N-like algorithm applied to the continuum model.

Efficient methods for the numerical approximation of the gradients or higher derivatives of various objective functions have been introduced in previous works. The Jacobian matrix F' of $F(\sigma, z) = R_{\sigma,z}I$ can be computed explicitly by sampling its rows using suitable variational formulations [40, 59]. Alternatively, matrix-free methods that avoid storing the full Jacobian but instead compute merely 'Jacobian times vector' evaluations, are possible; see e.g. [8, 20] for an adjoint operator technique that allows matrix-free computations.

3.3 Shape derivatives of the CEM electrode potentials

Shape optimization problems arise in many fields of science and engineering, including EIT. In the development of numerical shape optimization

methods, differentiation of a shape functional (or more generally a tensor) $J(\Gamma)$ with respect to perturbations of Γ plays a central role [17, 48].

There are several standard approaches to building numerical shape derivative based schemes. If the boundary is parametrized by a set of given functions, such as trigonometric functions or splines, a suitable shape derivative enables the use of standard optimization techniques, such as the Newton's method (3.3), for handling the free parameters in Γ. This parametric approach is straightforward to implement but it also has drawbacks, such as the inability to deal with changes in the topology (e.g. the emergence of holes or new domains). A more sophisticated framework is provided by *level set methods* [17], where boundaries are represented as level sets of auxiliary functions $\varphi : \mathbb{R}^d \times (0, \infty) \to \mathbb{R}$ so that $\Gamma_t = \{x \in \mathbb{R}^d \ : \ \varphi(x, t) = 0\}$. The level set methods can be used to build iterative numerical schemes where the evolution of Γ_t is determined by the (shape-derivative-dependent) non-linear level set equation for φ. Since no explicit geometry parametrization is required, flexibility with respect to topology changes is achieved.

Shape analysis (and related) concepts have been previously employed in EIT, but mainly to reconstruct inclusion shapes or other geometric entities lying well within Ω; see e.g. [25, 27]. In this thesis the main objective is to develop a practically applicable shape derivative with respect to the outer boundary Γ of the examined object, as well as with respect to the electrodes $\mathcal{E} = \{E_m\}_{m=1}^M$. The CEM provides an attractive framework for such considerations. Since both the injected currents and the measured voltages are discrete,

$$J(\Gamma, \mathcal{E}) = U(\Gamma, \mathcal{E}) = R_{\sigma,z}(\Gamma, \mathcal{E})I \tag{3.4}$$

is a natural choice for the shape tensor. Unfortunately, some subtleties are unavoidable due to the limited smoothness of the solution to (2.4); see the publications [**III**, **IV**] and the references therein.

Shape analysis of (3.4) can be carried out by perturbing the domain using suitable transformations, and keeping track of the variations in the shape tensor. The procedure can be summarized as follows. Consider perturbations of the identity having the form

$$\Phi_t(x) = x + tV(x), \quad x \in \overline{\Omega}, \quad t \geq 0, \tag{3.5}$$

which are diffeomorphisms for 'small enough' t and 'smooth enough' V (see e.g. **[I]**). Note, however, that the shape analysis can also be performed using more general domain transformations (see e.g. *the speed method* in [17, 48]). The values of the perturbed shape tensor (3.4) are $J(\Gamma_t, \mathcal{E}_t) = R_{\sigma,z}(\Gamma_t, \mathcal{E}_t)I$ where $\Gamma_t = \partial(\Phi_t(\Omega))$ and $\mathcal{E}_t = \{\Phi_t(E_m)\}_{m=1}^M$. Using some standard tools of the shape calculus for boundary value problems, namely the notions of *material and shape derivatives* [48], it can be shown that there exists $G_m(\Gamma, \mathcal{E}) \in \mathcal{D}'(\Gamma)$ acting as the *shape gradient* [17, 48] such that

$$\frac{\partial}{\partial t} J_m(\Gamma_t, \mathcal{E}_t)|_{t=0} = \langle G_m(\Gamma, \mathcal{E}), V|_\Gamma \rangle, \qquad m = 1, 2, \ldots, M \tag{3.6}$$

where $\langle \cdot, \cdot \rangle$ is a suitable dual evaluation. The explicit form of G_m depends on $J(\Gamma, \mathcal{E})$ as well as on certain (boundary operator evaluations of) the corresponding spatial potential $u = u(\Gamma, \mathcal{E})$. Unlike in some classical example problems, (3.6) not only depends on the component of $V|_\Gamma$ normal to Γ, but also — to account for the movement of the electrodes — on the tangential component of $V|_{\partial E}$ normal to ∂E; see e.g. [17] for more information on general structuring for classes of shape gradients.

Based on (3.6) it is possible to develop differentiability results that are well-suited for numerical applications: taking a vector field extension from Γ to $\overline{\Omega}$ with suitable continuity properties **[II]** yields the Fréchet differentiability of the electrode voltages $U = R_{\sigma,z}I$ with respect to sufficiently small vector fields living on Γ. In the case of regular enough parametrizations of Γ, this allows explicit formulas for the derivatives of U with respect to the parameters. However, this is not sufficient for our purposes since the positions of the electrodes $\mathcal{E}$ need also to be adjusted. Therefore, a separate derivative with respect to the movement of the electrodes is also of interest **[I]**. In fact, the evaluation of (3.6) for vector fields with $V \cdot \nu = 0$ on Γ turns out to be the correct interpretation for the electrode derivatives. This is a consequence of the fact that close-to-identity transformations with the property $\Phi(\overline{\Omega}) = \overline{\Omega}$ act almost as tangential perturbations in a relevant topology.

4. Summary of results

[**I**] In this paper, it is demonstrated that the measurement map of the CEM is Fréchet differentiable with respect to the electrodes. A general way of perturbing the electrodes is constructed using projections of vector fields living on the electrode boundaries. The Fréchet derivative is determined by the solution of an elliptic boundary value problem with distributional boundary conditions. A dual formula for the electrode shape gradient is derived, and employed in a Gauss–Newton algorithm for the simultaneous reconstruction of the conductivity and the electrode positions from simulated (noisy) measurement data.

[**II**] The analysis of [**I**] is modified to prove the Fréchet differentiability with respect to the outer boundary of the object. A dual formula for the boundary shape gradient is derived, and employed in the Gauss–Newton based reconstruction of the object cross-section along with other parameters [**I**]. The functionality of the algorithm is tested with simulated (noisy) measurement data.

[**III**] This article is an experimental validation of the reconstruction algorithm devised in [**II**]. The data are measured using a reshapable tank filled with tap water and conductive/resistive inclusions. An instability issue due to the small contact resistance is observed and circumvented by a suitable phasing of the reconstruction algorithm.

[**IV**] Theoretical grounds for the instability encountered in [**III**] are developed. It is shown that, when the contact resistances tend to zero, the interior CEM potential converges to a function without the regularity required by a dual formula used in the computations of [**III**]. As

a by-product, it is deduced that the electrode voltages of the CEM are more accurately Galerkin-approximated than the corresponding spatial potentials. Numerical experiments supporting these conclusions are presented.

[**V**] This article considers optimization of electrode positions with respect to certain (Bayesian) posterior covariance related criteria. To make the computations feasible, the CEM measurement operator is linearized with respect to the conductivity. The proposed optimization algorithm is of the steepest descent type, with the needed gradients computed based on a (second order) electrode shape derivative of the CEM. The functionality of the method is verified via two-dimensional numerical experiments.

Bibliography

[1] G. Alessandrini. Stable determination of conductivity by boundary measurements. *Appl. Anal.*, 27(1-3):153–172, 1988.

[2] K. Astala, M. Lassas, and L. Päivärinta. Calderón's inverse problem for anisotropic conductivity in the plane. *Comm. Partial Differential Equations*, 30(1-2):207–224, 2005.

[3] K. Astala, J. Mueller, L. Päivärinta, A. Perämäki, and S. Siltanen. Direct electrical impedance tomography for nonsmooth conductivities. *Inverse Probl. Imaging*, 5(3):531–549, 2011.

[4] K. Astala and L. Päivärinta. Calderón's inverse conductivity problem in the plane. *Ann. of Math.*, 163(1):265–300, 2006.

[5] A. B. Bakushinskii. The problem of the convergence of the iteratively regularized Gauss–Newton method. *Comput. Math. Math. Phys.*, 32(9):1503–1509, 1992.

[6] J. A. Barceló, T. Barceló, and A. Ruiz. Stability of the inverse conductivity problem in the plane for less regular conductivities. *J. Differential Equations*, 173:231–270, 2005.

[7] B. Blaschke, A. Neubauer, and O. Scherzer. On convergence rates for the iteratively regularized Gauss–Newton method. *IMA J. Numer. Anal.*, 17:421–436, 1997.

[8] L. Borcea. Electrical impedance tomography. *Inverse problems*, 18:R99–R136, 2002.

[9] R. Brown and R. Torres. Uniqueness in the inverse conductivity problem for conductivities witg 3/2 derivatives in L^p, $p > 2n$. *J. Fourier Anal. Appl.*, 9:1049–1056, 2003.

[10] M. Brühl and M. Hanke. Numerical implementation of two noniterative methods for locating inclusions by impedance tomography. *Inverse Problems*, 16(4):1029, 2000.

[11] A. Calderón. On an inverse boundary value problem. In *Seminar on Numerical Analysis and its Applications to Continuum Physics (Rio de Janeiro, 1980),* Soc. Brasil. Mat., pages 65–73.

[12] M. Cheney, D. Isaacson, J. C. Newell, S. Simske, and J. Goble. NOSER: An algorithm for solving the inverse conductivity problem. *Int. J. Imag. Syst. Tech.*, 2(2):66–75, 1990.

[13] M. Cheney, D. Isaacson, and J.C. Newell. Electrical impedance tomography. *SIAM Rev.*, pages 85–101, 1999.

[14] K.-S. Cheng, D. Isaacson, J. S. Newell, and D. G. Gisser. Electrode models for electric current computed tomography. *IEEE T. Bio-med. Eng.*, 36(9):918–924, 1989.

[15] R. Dautray and J.L. Lions. *Mathematical analysis and numerical methods for science and technology: Functional and Variational Methods*, volume 2. Springer-Verlag, 1988.

[16] K. Deimling. *Nonlinear functional analysis*. Springer-Verlag, 1985.

[17] M. C. Delfour and J.-P. Zolesio. *Shapes and Geometries: Metrics, Analysis, Differential Calculus, and Optimization*. SIAM, 2011.

[18] D. Dobson. Convergence of a reconstruction method for the inverse conductivity problem. *SIAM J. Appl. Math.*, 52:442–458, 1992.

[19] H. W. Engl, M. Hanke, and A. Neubauer. *Regularization of Inverse Problems*. Kluwer Academic Publishers, 1996.

[20] M. Gehre, T. Kluth, A. Lipponen, B. Jin, A. Seppänen, J. P. Kaipio, and P. Maass. Sparsity reconstruction in electrical impedance tomography: An experimental evaluation. *J. Comput. Appl. Math.*, 236:2126–2136, 2012.

[21] A. Greenleaf, M. Lassas, and G. Uhlmann. On nonuniqueness for Calderón's inverse problem. *Math. Res. Lett.*, 10(5/6):685–694, 2003.

[22] B. Haberman and D. Tataru. Uniqueness in Calderón's problem with Lipschitz conductivities. *Duke Math. J.*, 162(3):497–516, 2013.

[23] B. Harrach and J. K. Seo. Exact shape-reconstruction by one-step linearization in electrical impedance tomography. *SIAM J. Appl. Math.*, 42:1505–1518, 2010.

[24] L. M. Heikkinen, T. Vilhunen, R. M. West, and M. Vauhkonen. Simultaneous reconstruction of electrode contact impedances and internal electrical properties: II. Laboratory experiments. *Meas. Sci. Technol.*, 13:1855–1861, 2002.

[25] F. Hettlich and W. Rundell. The determination of a discontinuity in a conductivity from a single boundary measurement. *Inverse Problems*, 14(1):67, 1998.

[26] N. Hyvönen. Approximating idealized boundary data of electric impedance tomography by electrode measurements. *Math. Mod. Meth. Appl. S.*, 19(07):1185–1202, 2009.

[27] N. Hyvönen, K. Karhunen, and A. Seppänen. Fréchet derivative with respect to the shape of an internal electrode in electrical impedance tomography. *SIAM J. Appl. Math.*, 70(6):1878–1898, 2010.

[28] O. Imanuvilov, G. Uhlmann, and M. Yamamoto. The Calderón problem with partial data in two dimensions. *J. Amer. Math. Soc.*, 23(3):655–691, 2010.

[29] J. P. Kaipio, V. Kolehmainen, E. Somersalo, and M. Vauhkonen. Statistical inversion and Monte Carlo sampling methods in electrical impedance tomography. *Inverse Problems*, 16(5):1487, 2000.

[30] J. P. Kaipio and E. Somersalo. *Statistical and Computational Inverse Problems*. Springer-Verlag, 2004.

[31] C. Kenig, J. Sjöstrand, and Gunther Uhlmann. The Calderón problem with partial data. *Ann. of Math.*, pages 567–591, 2007.

[32] A. Kirsch. *An Introduction to the Mathematical Theory of Inverse Problems*, volume 120. Springer-Verlag, 1996.

[33] A. Kirsch and N. Grinberg. *The factorization method for inverse problems*. Oxford University Press, 2008.

[34] K. Knudsen, M. Lassas, J. Mueller, and S. Siltanen. Regularized D-bar method for the inverse conductivity problem. *Inverse Probl. Imaging*, 35(4):599, 2009.

[35] R. Kohn and M. Vogelius. Determining conductivity by boundary measurements. *Comm. Pure Appl. Math.*, 37(3):289–298, 1984.

[36] V. Kolehmainen, M. Lassas, and P. Ola. Inverse conductivity problem with an imperfectly known boundary. *SIAM J. Appl. Math.*, 66:365–383, 2005.

[37] M. Lassas and G. Uhlmann. On determining a Riemannian manifold from the Dirichlet-to-Neumann map. *Ann. Sci. Éc. Norm. Supér.*, 34(5):771–787, 2001.

[38] A. Lechleiter, N. Hyvönen, and H. Hakula. The factorization method applied to the complete electrode model of impedance tomography. *SIAM J. Appl. Math.*, 68:1097–1121, 2008.

[39] A. Lechleiter and A. Rieder. Newton regularizations for impedance tomography: a numerical study. *Inverse Problems*, 22(6):1967–1987, 2006.

[40] A. Lechleiter and A. Rieder. Newton regularizations for impedance tomography: convergence by local injectivity. *Inverse Problems*, 24(6):1065009, 2008.

[41] V. A. Morozov. *Regularization methods for ill-posed problems*. CRC Press, 1993.

[42] J. Mueller, S. Siltanen, and D. Isaacson. A direct reconstruction algorithm for electrical impedance tomography. *IEEE T. Med. Imaging*, 21(6):555–559, 2002.

[43] A. I. Nachman. Global uniqueness for a two-dimensional inverse boundary value problem. *Ann. of Math.*, pages 71–96, 1996.

[44] A. Nissinen, L. M. Heikkinen, V. Kolehmainen, and J. P. Kaipio. Compensation of errors due to discretization, domain truncation and unknown contact impedances in electrical impedance tomography. *Meas. Sci. Technol.*, 20(10):105504, 2009.

[45] A. Nissinen, V. Kolehmainen, and J. P. Kaipio. Reconstruction of domain boundary and conductivity in electrical impedance tomography using the approximation error approach. *Int. J. Uncertain. Quantif.*, 1:203–222, 2011.

[46] L. Päivärinta, A. Panchenko, and G. Uhlmann. Complex geometrical optics solutions for Lipschitz conductivities. *Rev. Mat. Iberoam.*, 19:57–72, 2003.

[47] O. Seiskari. *Analyticity of point measurements in inverse conductivity and scattering problems*. Aalto University publication series, DOCTORAL DISSERTATIONS 165/2013, 2013.

[48] J. Sokołowski and J.-P. Zolesio. *Introduction to Shape Optimization: Shape Sensitivity Analysis*. Springer-Verlag, 1992.

[49] E. Somersalo, M. Cheney, and D. Isaacson. Existence and uniqueness for electrode models for electric current computed tomography. *SIAM J. Appl. Math.*, 52:1023–1040, 1992.

[50] E. Somersalo, M. Cheney, D. Isaacson, and E. Isaacson. Layer stripping: a direct numerical method for impedance imaging. *Inverse Problems*, 7(6):899, 1991.

[51] S. Staboulis. *Fine tuning of the electrode positions in electrical impedance tomography.* University of Helsinki, Department of Mathematics and Statistics, 2010.

[52] J. Sylvester. An anisotropic inverse boundary value problem. *Comm. Pure Appl. Math.*, 43:201–232, 1990.

[53] J. Sylvester. A convergent layer stripping algorithm for the radially symmetric impedance tomography problem. *Comm. Partial Differential Equations*, 17(11-12):1955–1994, 1992.

[54] J. Sylvester and G. Uhlmann. A global uniqueness theorem for an inverse boundary value problem. *Ann. of Math.*, 125:153–169, 1987.

[55] A. N. Tikhonov and V. Arsenin. *Solutions of ill-posed problems.* Wiley, 1977.

[56] G. Uhlmann. Electrical impedance tomography and Calderón's problem. *Inverse Problems*, 25:123011, 2009.

[57] M. Vauhkonen, P. Vadász, A. Karjalainen, P., E. Somersalo, and J. P. Kaipio. Tikhonov regularization and prior information in electrical impedance tomography. *IEEE T. Med. Imaging*, 17(2):1487, 1998.

[58] P. J. Vauhkonen, M. Vauhkonen, T. Savolainen, and J. P. Kaipio. Three-dimensional electrical impedance tomography based on the complete electrode model. *IEEE T. Biomed. Eng.*, 46(9):1150–1160, 1999.

[59] T. Vilhunen, J. P. Kaipio, P. J. Vauhkonen, T. Savolainen, and M. Vauhkonen. Simultaneous reconstruction of electrode contact impedances and internal electrical properties: I. Theory. *Meas. Sci. Technol.*, 13:1848–1854, 2002.

[60] C. R. Vogel. *Computational Methods for Inverse Problems.* SIAM, 2002.

Aalto-DD 141/2014

ISBN 978-952-60-5862-7
ISBN 978-952-60-5863-4 (pdf)
ISSN-L 1799-4934
ISSN 1799-4934
ISSN 1799-4942 (pdf)

Aalto University

Department of Mathematics and Systems Analysis
www.aalto.fi

BUSINESS +
ECONOMY

ART +
DESIGN +
ARCHITECTURE

SCIENCE +
TECHNOLOGY

CROSSOVER

**DOCTORAL
DISSERTATIONS**